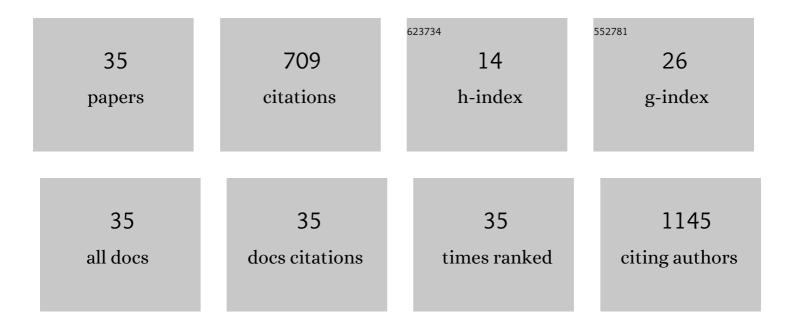
Zhi Wang

List of Publications by Year in descending order

Source: https://exaly.com/author-pdf/2720592/publications.pdf Version: 2024-02-01



#	Article	IF	CITATIONS
1	Series of in-fiber graphene supercapacitors for flexible wearable devices. Journal of Materials Chemistry A, 2015, 3, 2547-2551.	10.3	101
2	Three-dimensional graphene–polypyrrole hybrid electrochemical actuator. Nanoscale, 2012, 4, 7563.	5.6	86
3	A rationally-designed synergetic polypyrrole/graphene bilayer actuator. Journal of Materials Chemistry, 2012, 22, 4015.	6.7	66
4	Giant gauge factor of Van der Waals material based strain sensors. Nature Communications, 2021, 12, 2018.	12.8	62
5	Enhanced NO ₂ Sensitivity in Schottky-Contacted n-Type SnS ₂ Gas Sensors. ACS Applied Materials & Interfaces, 2020, 12, 26746-26754.	8.0	49
6	Photo-enhanced gas sensing of SnS ₂ with nanoscale defects. RSC Advances, 2019, 9, 626-635.	3.6	43
7	Effects of oxygen partial pressure on the structural and optical properties of undoped and Cu-doped ZnO thin films prepared by magnetron co-sputtering. Materials Letters, 2016, 164, 509-512.	2.6	25
8	Effects of oxygen/argon pressure ratio on the structural and optical properties of Mn-doped ZnO thin films prepared by magnetron pulsed co-sputtering. Surface and Coatings Technology, 2019, 357, 978-983.	4.8	24
9	Effects of sputtering and assisting ions on the orientation of titanium nitride films fabricated by ion beam assisted sputtering deposition from metal target. Materials Letters, 2016, 171, 304-307.	2.6	23
10	Probing thermal expansion coefficients of monolayers using surface enhanced Raman scattering. RSC Advances, 2016, 6, 99053-99059.	3.6	20
11	Structural and optical properties of ZnO thin films with heavy Cu-doping prepared by magnetron co-sputtering. Materials Letters, 2015, 143, 319-321.	2.6	19
12	Surface morphology evolution of CeO2/YSZ (001) buffer layers fabricated via magnetron sputtering. Applied Surface Science, 2013, 284, 150-154.	6.1	16
13	Plasmonic properties of titanium nitride thin films prepared by ion beam assisted deposition. Materials Letters, 2016, 185, 295-298.	2.6	16
14	Effects of nitrogen and oxygen partial pressure on the structural and optical properties of ZnO:N thin films prepared by magnetron sputtering. Materials Letters, 2016, 165, 123-126.	2.6	16
15	Structural and plasmonic properties of Ti Zr1â^'N ternary nitride thin films. Applied Surface Science, 2019, 476, 560-568.	6.1	16
16	Effects of substrate bias and temperature on the structure and dielectric properties of Ti Zr1â^'N ternary nitride thin films. Surface and Coatings Technology, 2019, 359, 258-264.	4.8	12
17	Stoichiometry-modulated dual epsilon-near-zero characteristics of niobium nitride films. Applied Surface Science, 2021, 537, 147981.	6.1	12
18	Effects of assisting ions on the structural and plasmonic properties of ZrN x thin films. Journal Physics D: Applied Physics, 2019, 52, 245102.	2.8	11

Zhi Wang

#	Article	IF	CITATIONS
19	Structural and dielectric properties of ion beam deposited titanium oxynitride thin films. Journal of Materials Science, 2019, 54, 1452-1461.	3.7	11
20	Modulation of the plasmonic characteristics of Ti-Zr ternary nitride thin films by assisting ions. Applied Surface Science, 2020, 505, 144579.	6.1	10
21	Study of substrate temperature and copper doping effects on structural, electrical and optical properties of Cu-doped and undoped ZnO thin films. Journal of Materials Science: Materials in Electronics, 2016, 27, 7822-7828.	2.2	9
22	Ion beam modification of plasmonic titanium nitride thin films. Journal of Materials Science, 2017, 52, 6442-6448.	3.7	9
23	Threshold magnetoresistance in anistropic magnetic 2D transition metal dichalcogenides. Journal of Materials Chemistry C, 2018, 6, 3058-3064.	5.5	9
24	Structural, Compositional, and Plasmonic Characteristics of Ti–Zr Ternary Nitride Thin Films Tuned by the Nitrogen Flow Ratio in Magnetron Sputtering. Nanomaterials, 2020, 10, 829.	4.1	9
25	Orientation selection in MgO thin films prepared by ion-beam-deposition without oxygen gas present. Nuclear Instruments & Methods in Physics Research B, 2015, 360, 60-63.	1.4	8
26	Surface enhanced Raman scattering on ion-beam-deposited <mml:math xmlns:mml="http://www.w3.org/1998/Math/MathML" altimg="si30.svg"><mml:mrow><mml:msub><mml:mrow><mml:mi mathvariant="normal">TiN</mml:mi </mml:mrow><mml:mrow><mml:mi>x</mml:mi></mml:mrow>substrates. Nuclear Instruments & Methods in Physics Research B, 2020, 472, 24-31.</mml:msub></mml:mrow></mml:math 	1.4 >> <td>6 1row></td>	6 1row>
27	Plasmonic properties of nonstoichiometric zirconium nitride, oxynitride thin films, and their bilayer structures. Physical Review Materials, 2021, 5, .	2.4	5
28	All-nitride broadband metamaterial absorbers. Results in Physics, 2022, 38, 105657.	4.1	5
29	An orientation competition in yttria-stabilized zirconia thin films fabricated by ion beam assisted sputtering deposition. Thin Solid Films, 2011, 520, 1115-1119.	1.8	4
30	A competition between (001) and (011) alignments in yttria stabilized zirconia thin films fabricated by ion beam assisted deposition. Physica C: Superconductivity and Its Applications, 2010, 470, 622-625.	1.2	3
31	Structural and optical properties of Cu–N codoped ZnO thin films deposited by magnetron cosputtering. Journal of Materials Science: Materials in Electronics, 2018, 29, 9901-9907.	2.2	2
32	Plasmonic characteristics of niobium nitride thin films modulated by assisting ions. Surfaces and Interfaces, 2021, 24, 101024.	3.0	2
33	Effects of arrival ratio and inclined angle on the orientation competition in ion beam assisting deposited yttria-stabilized zirconia thin films. Physica C: Superconductivity and Its Applications, 2012, 473, 57-60.	1.2	0
34	Effects of assisting ion energy and current on MgO films fabricated by ion-beam-assisted sputtering deposition. Materials Research Innovations, 2015, 19, S8-702-S8-704.	2.3	0
35	Characteristic modification by inserted metal layer and interface graphene layer in ZnO-based resistive switching structures. Chinese Physics B, 2018, 27, 027104.	1.4	0